Electronic Supplementary Material (ESI) for Biomaterials Science.

Supporting Information

for

Cysteine-Based Redox-Responsive Nanoparticles for Small-Molecule Agent Delivery

Liying Wang,‡ Xinru You,‡ Qi Lou,‡ Siyu He, Junfu Zhang, Chunlei Dai, Meng Zhao, Minyi Zhao, Hai Hu* and Jun Wu*

Table S1. The characteristics and applications of various small-molecule agents (SMAs).

SMA	Characteristics	Applications	Reference
Lapatinib	Dual tyrosine kinase inhibitor of epidermal growth factor receptor (EGFR) and human epidermal growth factor receptor 2 (HER-2); poorly soluble in water; easily incorporated with plasma protein.	Used in the treatment of advanced or metastatic breast cancer.	1, 2
Gefitinib	Orally-bioavailable tyrosine kinase inhibitor of EGFR; poorly soluble in water; easily incorporated with plasma protein.	Used in the treatment of non-small cell lung carcinoma (NSCLC).	3, 4
Crizotinib	ATP-competitive inhibitor of c-Met kinase; orally administered.	Used in the treatment of NSCLC.	5
Olaparib	Selective inhibitor of poly adenosine diphosphate-ribose polymeras-1 (PARP-1) and poly adenosine diphosphate-ribose polymeras-2 (PARP-2); poorly soluble in water; orally administered.	Used in the treatment of advanced ovarian cancer harboring BRCA mutations.	6
Everolimus	Inhibitor of mammalian target of rapamycin (mTOR); orally administered.	Used in the treatment of renal carcinoma and other tumors.	7
BYL719	Selective PI3Kα inhibitor; orally administered.	Used in the treatment of PI3Kα mutant cancers.	8

Synthesis and characterization of Cys-8E polymer

The Cys-8E polymer was synthesized by one-step polycondensation as previously reported.[9] Details of the procedure are as follows: first, 10 mmol of $(H\text{-}Cys\text{-}OMe)_2.2HCl$ and 15 mmol of triethylamine were mixed with 20 mL of DMSO, and then 10 mmol of sebacoyl chloride dissolved in 10 mL of DMSO was added dropwise into the mixture solution. After stirring for 15 min, the uniform mixture solution was precipitated in 250 mL of cold ethyl ether and then was dissolved in a little methanol. After precipitation in ethyl ether twice, the final product was dried in a vacuum oven at 45 °C. The chemical structure and physical properties of the Cys-8E polymer were characterized by various standard methods, including ^1H NMR, Fourier transform infrared spectroscopy (FTIR), gel permeation chromatography (GPC) and differential scanning calorimeter (DSC).

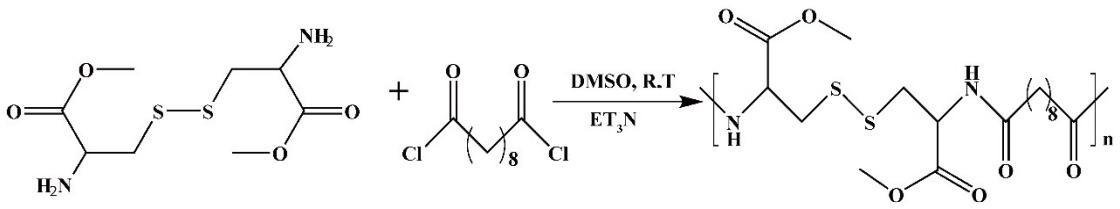

Figure S1. Synthetic route of Cys-8E polymer.

FTIR analysis

The Cys-8E polymer and KBr were mixed in a mass ratio of 1:100 and

pressed to tablet, following by the analysis of FTIR (VERTEX 70, Bruker, Germany).

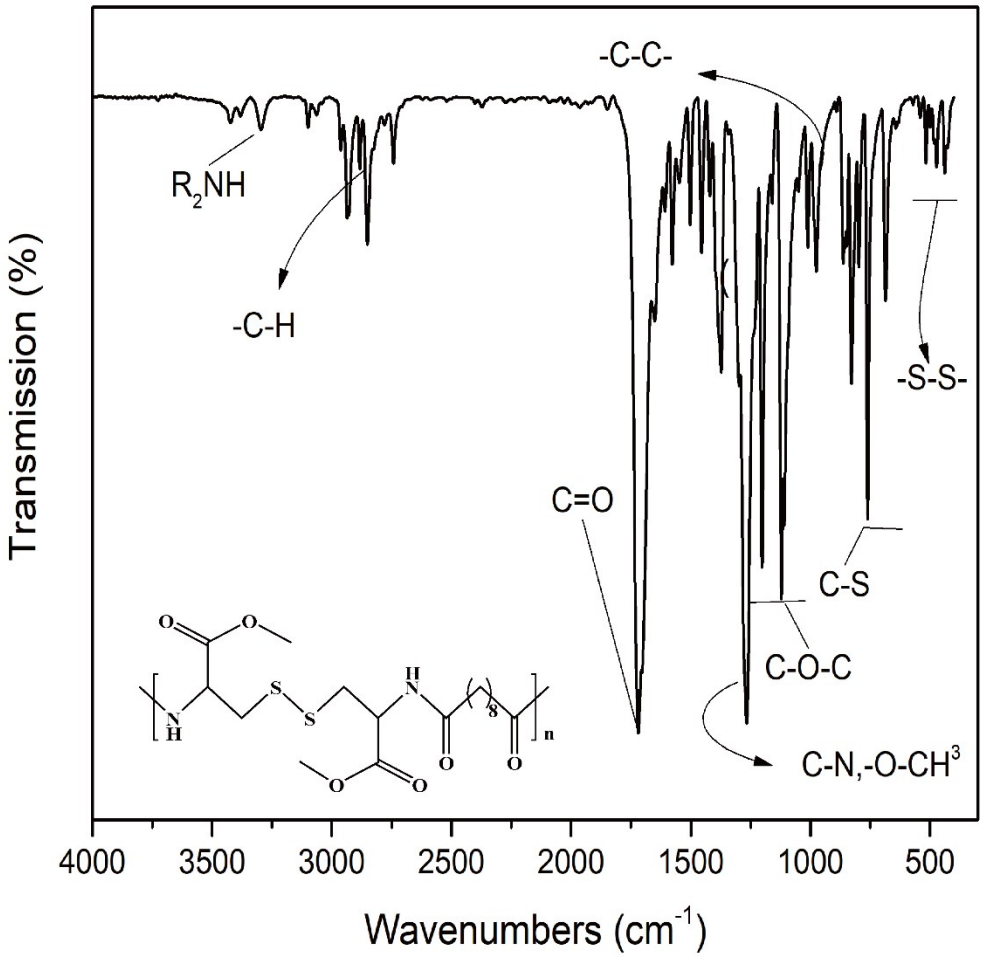

Figure S2. FTIR spectrum of Cys-8E polymer.

^{1}H MNR analysis

5 mg of Cys-8E polymer was dissolved in 500 μL Dimethyl Sulfoxide-

D6 and then was directly analyzed by MNR (Advance III, Bruker, Germany).

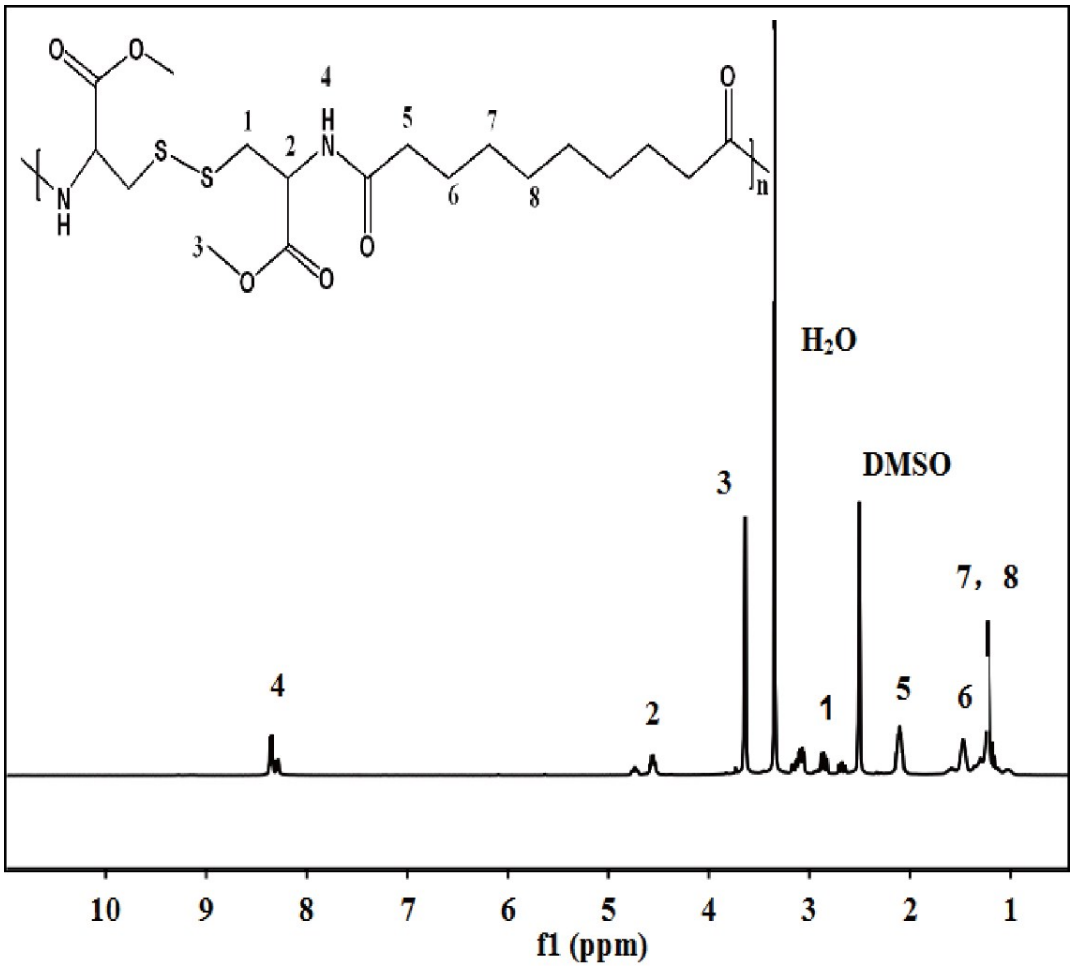

Figure S3. ^{1}H NMR spectrum of Cys-8E polymer.

GPC analysis

The Cys-8E polymer was dissolved in HPLC-grade DMF at a concentration of 1 mg/mL and then was directly analyzed by GPC (1260 Infinity, Agilent, USA) under a flow rate of 1 mL/min. Polystyrene standards were used for calibration.

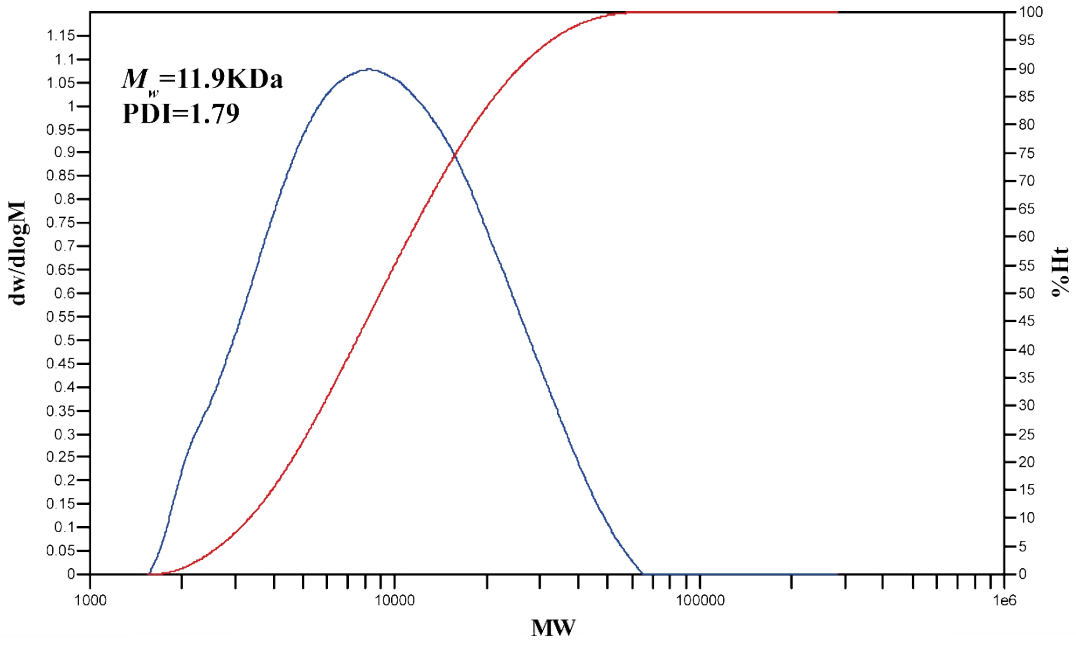

Figure S4. GPC distribution profile of Cys-8E polymer.

DSC analysis

DSC was applied to test the thermodynamic properties of the Cys-8E polymer. Briefly, approximately 5 mg of dry samples were placed in an aluminum pan, and the analysis was performed using DSC (Q20, TA, USA) with a scanning temperature range of -20 °C to 200 °C at a scanning rate of 10 °C/min under nitrogen flow.

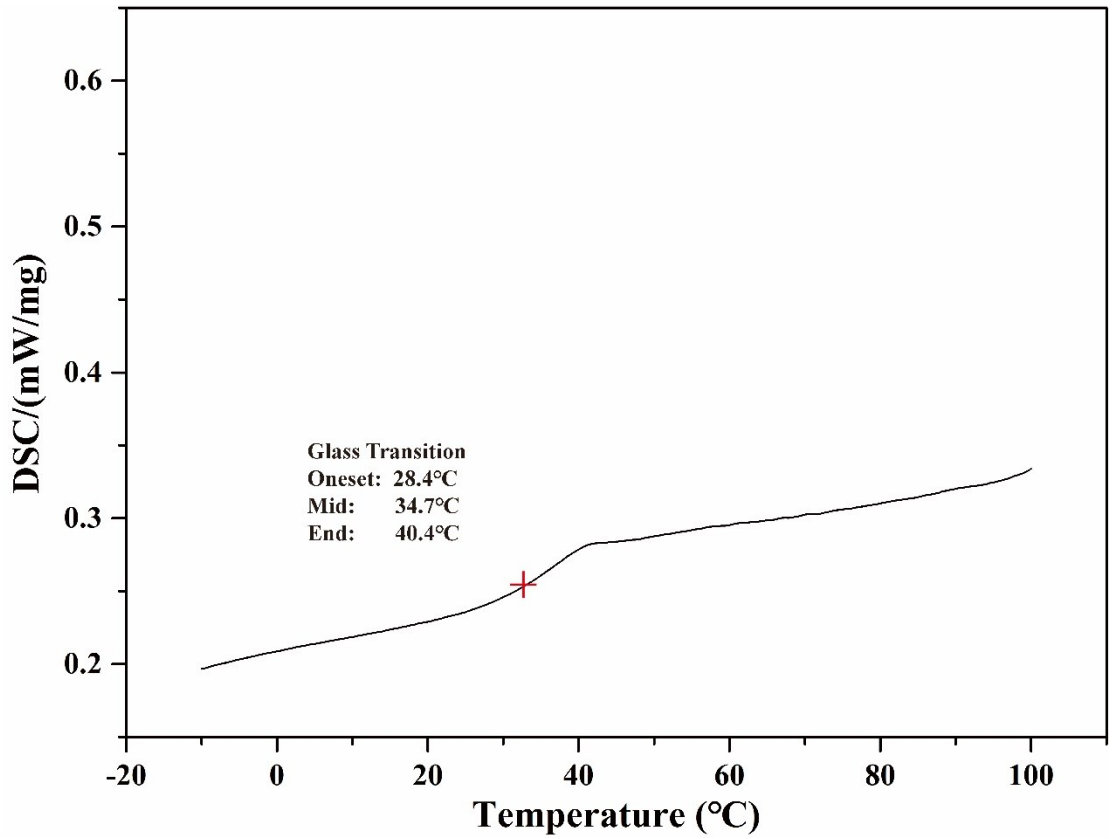

Figure S5. DSC curve of Cys-8E polymer.

TEM study

To visualize the morphology of Cys-8E NPs treated with 10 mM DTT for 30 min, 5 μL of NP solution (0.5 mg/mL) was carefully dropped onto the copper net and air dried at room temperature. Next, the NPs were negatively stained using 1% uranyl acetate solution for another 2 min. Finally, the morphology of NPs was observed by TEM (FEI, United States).

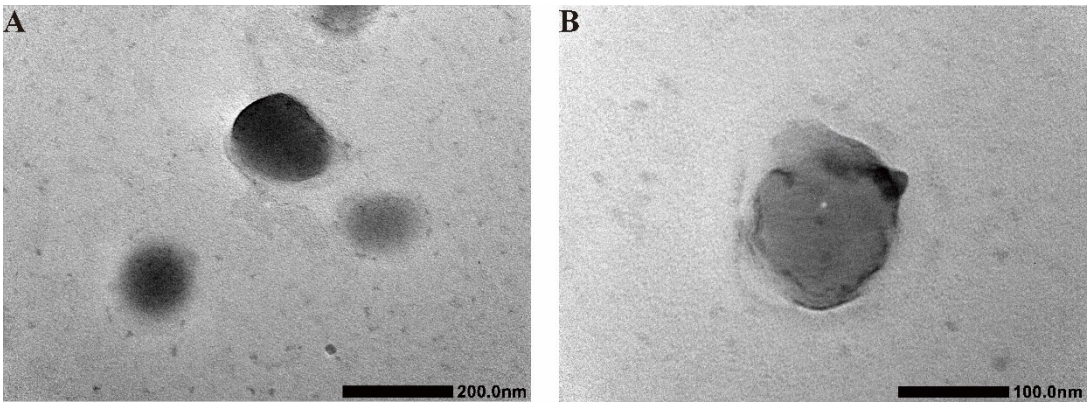

Figure S6. TEM images of Cys-8E NPs incubated with 10 mM DTT for 30 min. Scale bar: A, 200 nm; B, 100 nm.

Characterization of drug-loading capacity （DLC）

The DLC of various SMAs-NPs was determined using HPLC. In detail, a certain amount of SMA-NPs solution was mixed with HPLC-grade acetonitrile and then was placed in an ultrasonic machine for 1 h to produce the complete destruction of the NP structure. After centrifugation at 12,000 rpm for 15 min, the supernatant was withdrawn for analysis by an Agilent 1260 HPLC with a ZORBAX Extend-C18 column (4.5 × 15 mm, 2.7 μm). The detailed HPLC conditions of various SMAs are presented in Table S1.

Table S2. HPLC conditions of different SMAs.

SMA	**Gefitinib**	**Lapatinib**	**Everolimus**	**Crizotinib**	**BYL719**	**Olaparib**
ACN:H_2O	95:5	95:5	95:5	40:60	95:5	95:5
Flow rate (mL/min)	0.4	0.45	0.5	0.4	0.5	0.5
Injection	5 μL	10μL	5 μL	5 μL	5 μL	5 μL
Temperature	25 ℃	25℃	35 ℃	25℃	25℃	25℃
Wavelength	254 nm	210 nm	276 nm	254 nm	330nm	210nm
Rt (min)	3.155	6.732	6.26	4.059	5.295	6.196

MTT assay

The biocompatibility of Cys-8E NPs was determined via the MTT assay using 4T1 cells. 4T1 cells plated on 96-well plates were treated with serum-free medium containing Cys-8E NPs at different concentrations. After incubation for 24 h, 20 μL of MTT solution was added and incubated for 4 h. Next, all the medium was abandoned, and then 200 μL of DMSO was added into each well to shake for 5 min. Finally, the absorbance was measured by using a microplate reader.

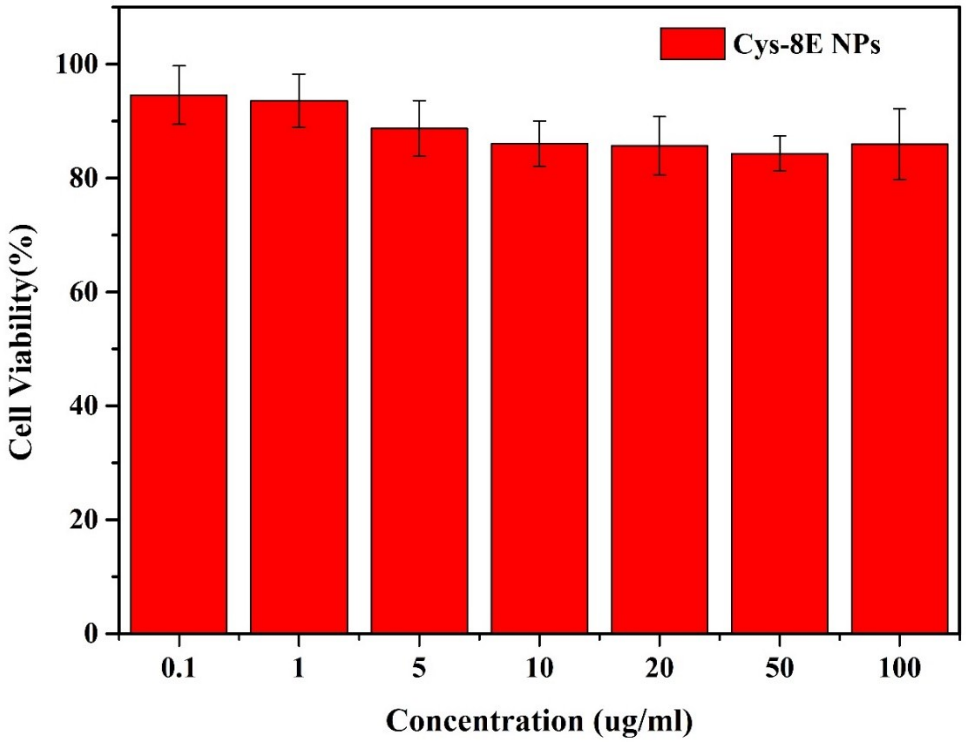

Figure S7. Cell viability of 4T1 cells treated with Cys-8E NPs for 24 h.

Reference

1 Z. A. Wainberg, A. Anghel, A. J. Desai, R. Ayala, T. Luo, B. Safran, M. S. Fejzo, J. R. Hecht, D. J. Slamon and R. S. Finn, *Clinical Cancer Research*, 2010, **16**, 1509-1519.

2 G. V. Bonde, S. K. Yadav, S. Chauhan, P. Mittal, G. Ajmal, S. Thokala and B. Mishra, *Expert Opin Drug Deliv*, 2018, **15**, 495-507.

3 X. L. Ni, L. X. Chen, H. Zhang, B. Yang, S. Xu, M. Wu, J. Liu, L. L. Yang, Y. Chen, S. Z. Fu and J. B. Wu, *Drug Deliv*, 2017, **24**, 1501-1512.

4 M. Ranson and S. Wardell, *Journal of Clinical Pharmacy and Therapeutics*, 2004, **29**, 95-103.

5 S. H. I. Ou, P. A. Janne, C. H. Bartlett, Y. Tang, D. W. Kim, G. A. Otterson, L. Crino, P. Selaru, D. P. Cohen, J. W. Clark and G. J. Riely, *Annals of Oncology*, 2014, **25**, 415-422.

6 U. Kortmann, J. N. McAlpine, H. Xue, J. Guan, G. Ha, S. Tully, S. Shafait, A. Lau, A. N. Cranston, M. J. O'Connor, D. G. Huntsman, Y. Z. Wang and C. B. Gilks, *Clinical Cancer Research*, 2011, **17**, 783-791.

7 T. Kawata, K. Tada, M. Kobayashi, T. Sakamoto, Y. Takiuchi, F. Iwai, M. Sakurada, M. Hishizawa, K. Shirakawa, K. Shindo, H. Sato and A. Takaori-Kondo, *Cancer Science*, 2018, **109**, 103-111.

8 C. Fritsch, A. Huang, C. Chatenay-Rivauday, C. Schnell, A. Reddy, M. Liu, A. Kauffmann, D. Guthy, D. Erdmann, A. De Pover, P. Furet, H. Gao, S. Ferretti, Y. Z. Wang, J. Trappe, S. M. Brachmann, S. M. Maira, C. Wilson, M. Boehm, C. Garcia-Echeverria, P. Chene, M. Wiesmann, R. Cozens, J. Lehar, R. Schlegel, G. Caravatti, F. Hofmann and W. R. Sellers, *Molecular Cancer Therapeutics*, 2014, **13**, 1117-1129.

9 J. Wu, L. Zhao, X. Xu, N. Bertrand, W. I. Choi, B. Yameen, J. Shi, V. Shah, M. Mulvale, J. L. MacLean and O. C. Farokhzad, *Angew Chem Int Ed Engl*, 2015, **54**, 9218-9223.